Since January 2020 Elsevier has created a COVID-19 resource centre with free information in English and Mandarin on the novel coronavirus COVID-19. The COVID-19 resource centre is hosted on Elsevier Connect, the company's public news and information website.

Biosensors and Bioelectronics 198 (2022) 113788

Contents lists available at ScienceDirect

Biosensors and Bioelectronics

journal homepage: www.elsevier.com/locate/bios

Electrochemical detection of ACE2 as a biomarker for diagnosis of COVID-19 and potential male infertility

Shuai Liu [a], Liping Han [b], Jinlong Li [c,*], Hao Li [d,**]

[a] Department of Urology, Shandong Provincial Hospital Affiliated to Shandong First Medical University, Jinan, Shandong, 250021, China
[b] Department of Neurology, Shandong Police Hospital, Jinan, Shandong, 250002, China
[c] Department of Laboratory Medicine, The Second Hospital of Nanjing, Nanjing University of Chinese Medicine, Nanjing, 210003, China
[d] School of Biological Science and Technology, University of Jinan, Jinan, 250024, China

ARTICLE INFO

Keywords:
SARS-CoV-2
COVID-19
Male infertility
Angiotensin converting enzyme 2
Covalent biosensing
Viral host target

ABSTRACT

Knowing how heavily the body is burdened by SARS-CoV-2 infection is all important to avoid tragic outcomes. This demands fast and convenient assays with minimum requirement for instruments and reagents. Therefore, a short synthetic peptide is developed to perform direct serum assay, using portable hand-held potentiostat, in a reagent-less manner. The target is angiotensin converting enzyme 2 (ACE2), a protein secreted by the body into the blood to restrict viral invasion. Specifically, under electrochemical potential scanning, the peptide can covalently capture ACE2 from the serum, and then form a covalent gel-like 2D protein network with the serum proteins, in an ACE2-specific fashion. This formation of a covalent biosensing complex enables sensitive detection in serum samples of SARS-CoV-2 infected patients. The detected serum level of ACE2 can not only serve as an index of viral load, but may also hint at the associated risk of potential male infertility. These results may point to field application of this simple design in the clinical practice in treating COVID-19 in the near future.

1. Introduction

Since the pandemic outbreak of COVID-19, the work load of hospital staff around the world has grown exponentially (Mehta et al., 2021; Theorell, 2020). Working under constant emotional stress (Prasad et al., 2021), operating complicated and expensive equipment (Feingold et al., 2021), and charged with the task to make decisions according to the ever-changing situation (Morgantini et al., 2020), they soon descend into a state of mental fatigue (Sasangohar et al., 2020). Human errors start to appear (Di Trani et al., 2021), sometimes leading to fatal consequences (Vandenberg et al., 2021). Simpler biomedical assays using less complicated instrument can significantly alleviate the burden of the medical staff. Electrochemical analytical devices are currently a hot spot for achieving such simplicity. For example, screen printed electrode (García-Miranda Ferrari et al., 2021) coupled with hand-held potentiostat (Abdullah et al., 2019) can now do some of the analytical works directly on-site, replacing the large instruments sitting in the clinical laboratory. But these portable bio-analysis devices also demand simpler assay designs. Those assay designs with multiple steps for adding expensive reagents such as antibodies, enzymes and nonmaterial may compromise the inherent advantage of these portable and compact devices. Indeed, since the outbreak, many relevant fields have achieved progress in combating the virus, such as the diagnostics of COVID-19, evaluation of specific protein-protein interactions of SARS-SARS-CoV-2 proteins with other proteins, as well as some newly developed methods for the determination of specific RNA sequences of SARS-CoV-2 (Drobysh et al., 2021; Dronina et al., 2021; Plikusiene et al., 2021).

In this work, using simple synthetic chemical probes whose behavior can be electrochemically fine-tuned, an assay for predicting the viral load of SARS-CoV-2 has been developed. In this design, all the biosensing procedures, including signal amplification, can be completed in the clinical serum sample solution. No other reagents, apart from the biosensing electrode, is needed during the detection process. Specifically, the viral marker protein to be assayed is the angiotensin converting enzyme 2 (ACE2), which is now well known to act as the cell membrane entrance for the virus particle (Gheblawi et al., 2020). The virus particles mainly attack epithelial cell lined ducts, since these cells constitutively express high levels of ACE2 (Guney and Akar, 2021). The pulmonary ducts are not the only victim, (Sungnak et al., 2020), the

* Corresponding author.
** Corresponding author.
E-mail addresses: jinlonglilab@njucm.edu.cn (J. Li), chem_lihao@163.com (H. Li).

https://doi.org/10.1016/j.bios.2021.113788
Received 27 July 2021; Received in revised form 8 November 2021; Accepted 11 November 2021
Available online 19 November 2021

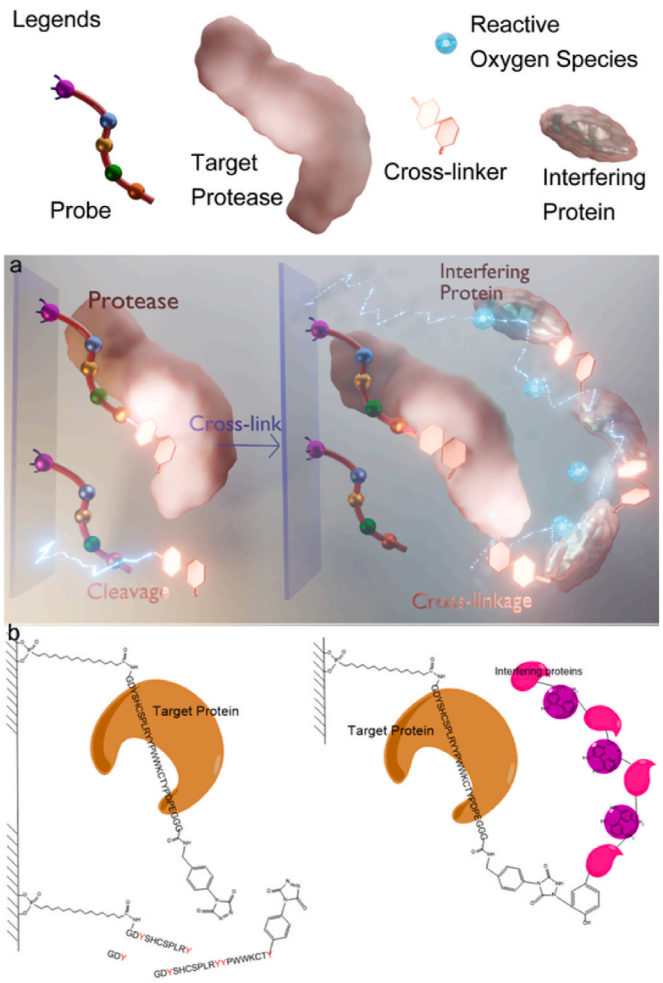

Scheme 1. The proposed method for detecting ACE2 in serum. (a) is the rendered cartoon, while (b) is the schematic.

male regenerative organs are also liable (Li et al., 2020a), as these are full of ACE2 over-expressed epithelial cells, making SARS-CoV-2 infection looking like a real risk of male fertility (Cardona Maya et al., 2020; Chen and Lou, 2020). To limit viral entry via cell membrane ACE2 and the above associated risk of infertility, the human body elevates the serum level of ACE2 as a defensive measure. Therefore, as indicated by some recent clinical reports, serum ACE2 may serve as the index of viral load and the associated complications.

In the design, as shown in Scheme 1, the synthetic probe for detecting ACE2 is tethered on the screen printed electrode surface. This probe is a short peptide sequence that can specifically recognize ACE2, with nano-molar affinity (Huang et al., 2003). But peptide-ACE2 binding does not lead to any readable electrochemical I–V signal readout, and certain mechanism of signal conversion is needed. Since no additional reagents are allowed to enter the biosensing system. The electrochemical device seems to be the only means for signal conversion. So a well-tried method previously employed for sample pre-treatment in mass spectra and liquid chromatography is used: electrochemical scanning between 0.5 and 1 V can cut peptide strand at the carboxyl end of tyrosine moieties (Permentier and Bruins, 2004), while the probe peptide for ACE2 coincidentally contains this amino acid. At the same time, the probe-ACE2 molecular recognition also brings the tyrosine moieties on the probe and on the target protein close together. And tyrosine cross-linking through the same electrochemically agitated reactive oxygen species (ROS)-mediated pathway (Larios et al., 2001) is also likely to take place between the probe and the target protein. So, the ACE2-free probe molecules on the electrode surface may be discomposed electrochemically, while the ACE2-bound probe molecules may be protected by the partial decomposing of the captured target protein "shielding" the probe from the ROS. In this way, on the one hand, the target protein molecules are covalently immobilized on the electrode surface; on the other hand, all the protein-free probe molecules lose their functional groups to the solution phase.

This special functional group, phenyl-urazol (Alvarez-Dorta et al., 2018), can generate amplified signal, through interacting with all the non-specific interfering serum proteins (mainly albumin). By the above cutting of all these two-headed phenyl-urazol groups into the serum, these cross-linking reagents "released" from the electrode surface can intermingle with the serum proteins. And then, electrochemical scanning over another potential range can induce these cross-linkers to connect with the tyrosine groups on the interfering serum protein molecules, forming a network of proteins. This gel-like formation can be anchored to the electrode surface by the ACE2 proteins already covalently captured there by the previous step. Since all the ACE2-free probes on the electrode have already lost their tyrosine residuals, the protein network can only use the target protein molecules as its foothold points on the surface. So that, higher ACE2 concentration in the serum sample can lead to more gel-like network being retained on the electrode surface, after thorough rinsing. Then, the de-natured proteins can generate amplified signal readout proportional to ACE2 abundance, through the electrochemical oxidation of aromatic amino acids exposed by rinsing. The proposed method has been successfully applied in detecting the blood sample of SARS-Cov-2 infected patients, showing the potential as a clinical early screening method for the virus in the near future.

2. Experimental section

2.1. Chemical and biological materials

The proposed probes, of which the chemical structure was shown in Scheme 1, was custom-synthesized by Science Peptide, Shanghai, as freeze-dried powder, purity >95%. The powder was dissolved with 100 mM phosphate buffered saline (PBS), pH = 7.4, to a concentration of 20 μM, as the stock solution. The human recombinant ACE2 was from R&D system, received as a filtered tris buffer, ACE2 concentration: 200 μM. It was diluted with the above PBS above to a stock solution, with ACE2 at 100 nM. SARS-Cov-2 ELISA assay kit (Elecsys® Anti-SARS-CoV-2 kit) was from Roche, and used following the instruction of the provider. Human recombinant serum albumin was from Albumedix, while human recombinant thrombin was from R&D system. All the stock solutions of the synthetic probe and target proteins were sub-packaged into batches of small vials, to ensure that each vial was just enough for single use, so that freeze-thaw cycles could be completely avoided. All the other reagents were of analytical grade. And the double distilled water for preparing the above solutions was prepared using a MiliQ water purification system, and was purified to a specific conductivity of 18 MΩ/cm. Serum had also been collected from a healthy volunteer for preparing standard samples as detailed below. The clinical samples of serum fractionated from periphery blood of hepatocellular carcinoma patients were retrieved from the sample bank of the biosafety level P2.5 clinical laboratory of Nanjing Second Hospital, with elected consensus by the local ethical committee.

2.2. Fabrication of the sensing surface for detecting the target protein

Conductive Indium Tin Oxide (ITO) coated glass was cut to small pieces. For probe immobilization, the ITO glass slide was serially immerged in dd water, ethanol and methanol for bath-supersonicating to remove any organic impurities absorbed on its surface. After bath-sonicating, the slide was thoroughly rinsed with dd water, before being brought to probe modification. The probe contained, at one of its ends, 16-Phosphohexadecanoic acid residuals (Sigma-Aldrich) for self-assembling on the surface of ITO (Chockalingam et al., 2014). To

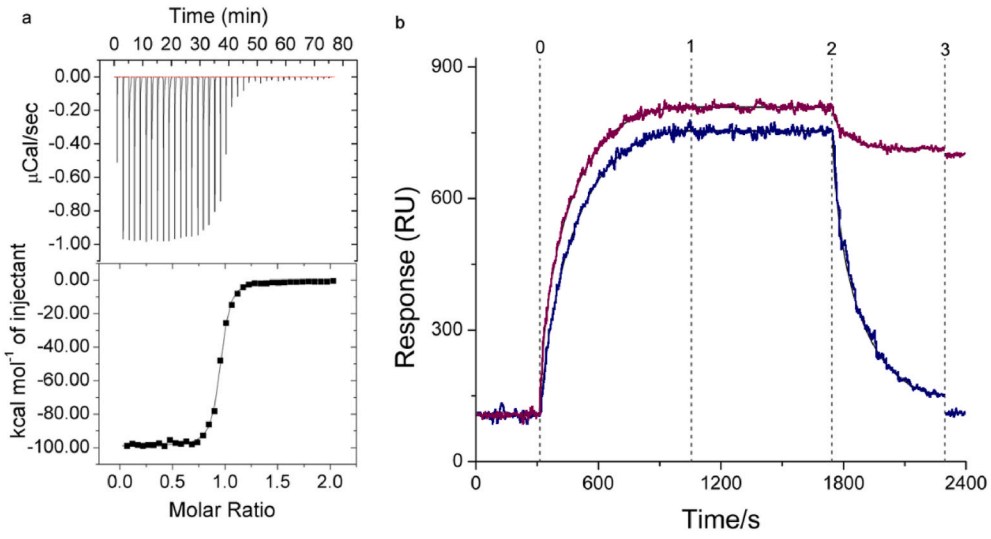

Fig. 1. Characterization of the non-covalent (a) and covalent (b) interaction of the designed probe and the target protein ACE2. (a) Isothermal titration calorimetry studying the molecular recognition between the probe and ACE2, obtained by titrating 0.1 mM probe into 0.01 mM ACE2, the buffer solution is the standard PBS buffer, the buffer is degassed before experiment. The upper row is the raw data, the lower row is the binding curve obtained by integrating the peak area of the row data, and then fitted to a 1:1 binding model. (b) Surface plasma resonance time course of surface immobilized probe interacting with ACE2. The blue line is a control without electrochemical scanning. Specifically, different concentrations of ACE2 in 10 mM PBS were separately pumped into the flow cell at a flow rate of 180 μ l/min using a mini-pump (Longer, T60-S2&WX10-14, dimensions: 107 × 60 × 80 mm, weight: 450 g). For each assay, the volume of ACE2 sample is 1 mL. The relative intensity increased significantly due to ACE2 binding specifically to probes on the sensing surface, and the values of the relative intensity were recorded and plotted as a function of time. Then, mild surfactant was pumped into the flow cell to remove unbound ACE2 molecules. Urea solution (2.0 M) was then used to strip the surface-bound ACE2 and effectively regenerate the sensing surface. The numbered points 0 to 3 represents the start of adding ACE2 (33 nM), the beginning of electrochemical scanning, the adding of mild surfactant, and the adding of de-naturing detergent.

initiate this process, the stock solution of the probe was dropped on the slide just cleared, and the area covered by the drop of stock solution was then marked out with a mark pen. The self-assembling process was then allowed to proceed for 16 h at 4 °C in a refrigerator under darkness. The slide was finally rinsed with copious amount of dd water and dried under a stream of high purity nitrogen, before being sent to detect the samples.

2.3. Detection of standard and clinical samples using the proposed method

The slide was used for the interface measurements, namely, the surface plasma resonance and the electrochemical measurements. The samples to be detected came in three different types. The first was the "standard" sample diluted with PBS buffer. The second type was the "serum" sample diluted with the serum of the healthy volunteer. The third kind of sample was the serum from the clinically collected blood. For the standard and serum samples, recombinant ACE2 was employed, for simple quantification, the stock solution of ACE2 was directly diluted. To detect these samples, they were dropped onto the slide, inside the marked-out area, and the mixture was incubated at ambient temperature for proper time as described in the results and discussion. In the detection, after incubation with the sample, current was run through the conductive slide for electrochemical scanning from 0.5–1 V at a voltage scan rate of 0.1 V/s for 10 min, to initiate the electrochemical cleavage of the substrate probe. Then the slide was subject to a second step of electrochemical scanning −0.3–0.9 V to initiate the tyrosine click chemistry, in the presence of 10 μM urazol cross-linker.

2.4. Experimental measurements of the detected signal readout

The MicroCal ITC200 system (GE Healthcare Life Sciences) was used for isothermal titration calorimetry (ITC) measurement. The titration was performed at 25 °C. The titration schedule consisted of 38 consecutive 1 μL injections with at least 120 s between each two injections. The heat of dilution measured by titrating over saturation from each data set was subtracted. Before titration, all solutions were degassed. Origin 7.0 software was used to analyze the data. The electrochemical measurement was carried out on a CHI660D potentiostat (CH Instruments) with a conventional three-electrode system: the glass slide was used as the working electrode, the saturated calomel electrode (SCE) was used as the reference electrode, and the platinum wire was used as the counter electrode. The electrolyte vial is a self-made type of approximately 100 μL. Parameters of electrochemical measurements: technique, square wave voltammetry; potential increment, 0.004 V; potential amplitude, 0.025 V. The SPR measurement was performed by an Autolab ESPRIT system (Echo Chemie B.V., The Netherlands) equipped with a 670 nm monochromatic p-polarized light source. It was noted that this model was also capable of simultaneously performing simple electrochemical measurements, meaning that it had an integrated potentiostat module. Specifically, different concentrations of ACE2 in 10 mM PBS were separately pumped into the flow cell at a flow rate of 180 μ l/min using a mini-pump (Longer, T60-S2&WX10-14, dimensions: 107 × 60 × 80 mm, weight: 450 g). For each assay, the volume of ACE2 sample is 1 mL. Then, mild surfactant was pumped into the flow cell to remove unbound ACE2 molecules. Urea solution (2.0 M) was then used to strip the surface-bound ACE2 and effectively regenerate the sensing surface. A QM-4/2005 fluorescence spectrometer (Photon Technology International, Inc., Birmingham, NJ) equipped with a xenon lamp was used to measure the fluorescence emission spectrum of the surface. The light source and the detector were located on the same plane and were at right angles to each other. The glass slide was kept in a water-filled test tube at 60° from the bottom of the test tube for fluorescence measurement. The surface with the gold film should be away from the light source and towards the detector. The activation peak wavelength of di-tyrosine was 325 nm, of Amplex red, was 570 nM. The Atomic force microscopy (AFM) images are recorded using Agilent 5500 AFM system. Samples were imaged at a scan rate of 0.5–1 Hz in a tapping mode. AFM tips with resonant frequency in a range 160–260 kHz were used. Images were acquired at a resolution of 512 × 512 pixels.

3. Results and discussion

3.1. Validation of the proposed non-covalent tandem covalent capturing of the target protein using various methods

First, the designed probe is studied to verify its ability to specifically target ACE2. In the design, the non-covalent molecular recognition between the peptide probe and ACE2 first brings the two together, and then electrochemical potential scanning induces the cross-linking

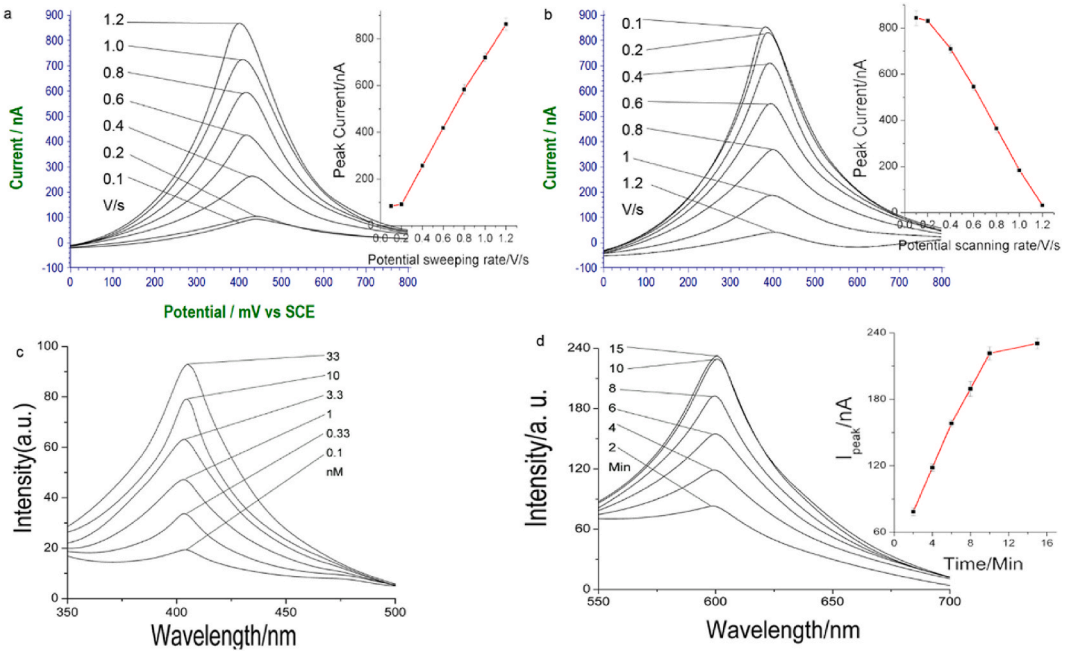

Fig. 2. Electrochemical and fluorescent characterization of the electrochemically controlled cleavage and cross-coupling in the biosensing process. (a) Ferrocene electrochemical signal recorded on the sensing surface representing a time course of electrochemical scanning between 0.5 and 1 V applied to the sensing surface in the absence of any ACE2. The inset plots the current peak responses against electrochemical scanning rate, the error bars represent the standard deviation (n = 3). Parameters of electrochemical measurements: technique, square wave voltammetry; potential increment, 0.004 V; potential amplitude, 0.025 V. (b) Similar ferrocene signal recorded in the electrolyte solution during electrochemical scanning. The meaning of curves and points are the same as (a). (c) Fluorescent signal of di-tyrosine product recorded on the sensing surface, after 10 min of electrochemical potential scanning the same as in (a) and (b). The concentrations of ACE2 used are marked on the graph. (d) Fluorescent signal of amplex red recorded as a time course representing the evolution of reactive oxygen species on the sensing surface. Surplus amplex red (1 μM) is added during the electrochemical scanning the same as in (a)–(c), while 0.1 μM horse radish peroxidase is also present, so the reactive oxygen species generated on the electrode, in the absence of any ACE2.

between the two molecules. So, the molecular recognition is first tested, using isothermal titration calorimetry (ITC), this method measures the heat of reaction when the probe recognizes and interacts with the target protein. More probes will gradually saturate a certain amount of target protein, giving rise to saturation curve. As shown in Fig. 1a, a typical saturated binding curve can be observed, indicating relatively strong binding between the probe and ACE2, confirming that the ACE2-targeting ability of the original peptide has not been compromised by adding the cross-linker group. ITC is conducted in the solution phase, so the behavior of the designed probe on the sensing surface is then studied using surface plasma resonance (SPR). This unique phenomenon can only be triggered at certain angle of incident for certain sensing surface. Binding of the target protein will alter the index of refraction of the sensing surface, giving rise to larger SPR signal. This signal can be plotted against time to give a time course as shown in Fig. 1b. As shown in Fig. 1b, the red curve represents the experiment using the designed probe to first non-covalently capture the target protein ACE2 from the solution phase (point 0), and then, electrochemical scanning is added to induce covalent capturing of ACE2 (point 1), before mild surfactant (point 2) and denaturing detergent (point 3) are added in tandem. More details on interpreting the SPR signal is described in the supporting information (Page S2).

To gain an in-depth view of the electrochemically facilitated target recognition process, electrochemical cleavage of ACE2-free peptide and cross-linking of ACE2-bound peptide need to be studied more directly. For this purpose, the phenyl-urazol end group of the peptide probe is replaced by the commonly used electrochemical signal reporter ferrocene. Then, a peptide probe modified electrode is directly subject to electrochemical potential scanning in the absence of the target protein. After gradually longer time of scanning, the electrode is transferred to another blank electrolyte buffer, and ferrocene signal is detected from both the electrode and the solution for the cleavage step. As shown in Fig. 2a and b, the variation of peak signal strength with respect to scanning time on the electrode and in the surface show reciprocal trends: while ferrocene signal gradually decreases on the electrode surface, it nonetheless keeps increasing in the solution. This may confirm that the electrochemical cleavage can detach the end group of the designed probe into the solution phase as expected.

In the presence of target ACE2 molecules, the formation of covalent cross-linkage between the probe and the target protein can be directly monitored fluorescently since the tyrosine to tyrosine cross-linking can form a di-tyrosine product with fluorescent emission. But for this experiment, screen printed electrode is temporarily replaced by a transparent ITO glass slide for fluorescent measurement on the sensing surface. After incubation with the ACE2 solution sample, and electrochemical potential scanning in the presence of the sample liquid drop, the sensing slide is then put into the cuvette of fluorescent measurement, obtaining the characteristic fluorescent signal of di-tyrosine, as shown in Fig. 2c, which is proportional to the amount of ACE2 contained in the sample. The proposed reaction mechanism is detailed in the supporting information (Page S2). To more directly study this mechanism, amplex red dye is employed to record the time course of ROS generation when electrochemical scanning is applied to the sensing surface. And as shown in Fig. 2d, more and more ROS represented by the fluorescent signal of ROS oxidized amplex red can be observed on the electrode surface during potential scanning. The surface density of the probes and the time course of covalent interaction are studied using this ferrocene tagged probe (Fig. S1 and Fig. S2).

3.2. *Improving the sensitivity of detecting the target protein by electrochemical cross-linking*

Under these optimized conditions, the next step is to use the electrochemical potential scanning to induce cross-linking between the

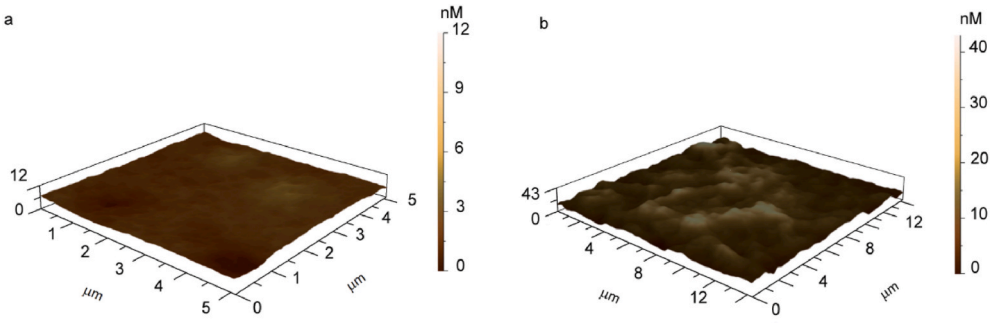

Fig. 3. Atomic force microscopic images of the sensing surface before the sensing process (a), and after the two steps of electrochemical scanning (b). The Atomic force microscopy (AFM) images are recorded using Agilent 5500 AFM system. Samples were imaged at a scan rate of 0.5–1 Hz in a tapping mode. AFM tips with resonant frequency in a range 160–260 kHz were used. Images were acquired at a resolution of 512 × 512 pixels.

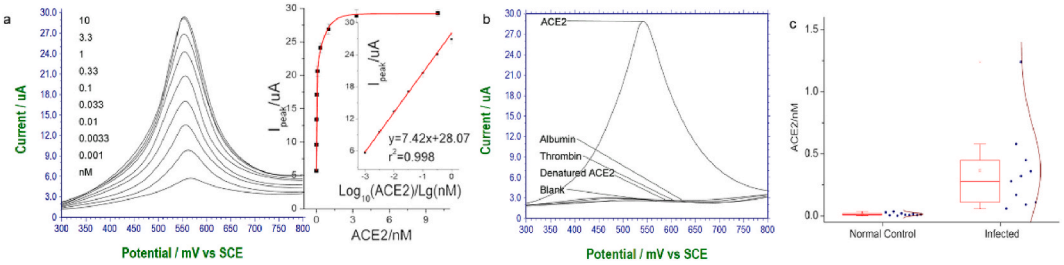

Fig. 4. Analytical performance of the proposed method in detecting serum-diluted and clinical serum samples. (a) The electrochemical peak responses of aromatic amino acids of the cross-linked proteins on the sensing surface. Inset is the peak responses plotted as a function of ACE2 concentration. The linear relationship between the peaks and the logarithm of ACE2 concentration has also been included. The error bars represent the standard deviation (n = 3). (b) The specificity with respect to major interfering proteins contained in the serum sample. (c) Box charts showing the detection of clinical serum samples of SARS-Cov-2 infected patients with a control using serum samples of healthy volunteers.

target protein and various serum interfering proteins. For this purpose, the above standard ACE2 sample prepared by diluting with standard PBS buffer is replaced by the serum of a healthy volunteer, while the ferrocene tagged probe is replaced by the designed probe that can release phenyl-urazol cross-linkers after electrochemical scanning. Then, after simple incubation and two subsequent steps of electrochemical scanning in the presence of the sample liquid drop, one between 0.5 and 1 V, and a second electrochemical scanning between −0.3-0.9 V, the surface of the electrode is examined by atomic force microscopic (AFM) method. As shown in Fig. 3a, a dense network-like morphology can be observed on the surface, while a relatively flatter surface can be observed after simple incubation but without electrochemical scanning (Fig. 3b). Cathodic stripping signal is then employed to amplify the readout, as shown in Fig. S3 and Fig. S4.

3.3. Analytical performance in detecting the target protein in serum spiked sample and clinical samples

Then, quantitative detection of ACE2 in serum diluted sample is performed. As shown in Fig. 4a, gradual increase of electrochemical current peak signals can be recorded in detecting higher and higher concentrations of ACE2, directly in serum. And a working can be established with a linear range between the signal readout and the logarithm of ACE2 concentration. The standard deviation of all measurements (n = 3) is below 5%. Shown in Fig. 4b is the specificity with respect to serum interfering species, and it can be seen that only the target protein can induce observable signal readout. Major serum proteins such as albumin, globulins and fibrinogen have been tested, as shown in Fig. S5, and their interfering effect is negligible. Periphery blood sample from SARS-CoV-2 infected patients are collected and detected using the proposed method. As shown in Fig. 4c, the level of ACE2 detected is 30–50 times higher than that in the healthy volunteers. The recent understanding of how SARS-CoV-2 invades the host cells bring about a serious concern about the potential damage to male regenerative functions of SARS-CoV-2 infection (Li et al., 2020b). Mounting evidences are suggesting that testicular tissue is particularly vulnerable to this virus (Ma et al., 2021), and not only testicular pain is an unusual presentation of COVID-19 (La Marca et al., 2020), the alteration of testicular tissue by viral infection may lead to impairment of spermatogenesis (Zafar and Li, 2020), not to mention the risk of contracting SARS-CoV-2 through intercourse (Patrì et al., 2020). Therefore, the serum level of ACE2 detected using the proposed method may be an index of these associated risks of COVID-19 (Nagy et al., 2021). It is worth noting that COVID-19 affects different people in different ways, clinical manifestations range from coughing and tiredness to severe symptoms such as difficulty in breathing. Future works will focus on discriminate such difference in viral load using the propose method, and on improving the sensitivity of detection beyond that of the commercially available antibody-based methods (Table S1).

4. Conclusion

In this work, a method for directly assaying a host marker protein of COVID-19 in the periphery blood of SARS-CoV-2 infected patients has been developed. In this method, using only a short peptide sequence that can specifically target ACE2, a glass slide or a screen-printed electrode chip is able to detect the protein in serum, with decent signal amplification enabling a limit of detection in serum as low as 1 pico-molar. Using this method, the clinical serum sample of SARS-Cov-2 infected patients can be directly detected, without using any complicated and expensive fixed instruments. These results may point to the application of the proposed method in risk-evaluation of SARS-CoV-2 infection.

Author statement

Shuai Liu was responsible for the conception of the study and wrote

the manuscript.

Liping Han contributed significantly to the experiment and preparation of the manuscript.

Jinlong Li reviewed the manuscript and provided the clinical samples.

Hao Li contributed significantly to the experiment and preparation of the manuscript.

Declaration of competing interest

The authors declare that they have no known competing financial interests or personal relationships that could have appeared to influence the work reported in this paper.

Acknowledgement

We would like to thank the Natural Science Foundation of China (81602227), the Municipal Science and Technology Project of Jinan (201907037), the Provincial Promotion Plan for Biomedical and Pharmaceutical Research of Shandong (202004051394).

Appendix A. Supplementary data

Supplementary data to this article can be found online at https://doi.org/10.1016/j.bios.2021.113788.

References

Abdullah, S., Tonello, S., Borghetti, M., Sardini, E., Serpelloni, M., 2019. J. Sensors 2019, 6729329.
Alvarez-Dorta, D., Thobie-Gautier, C., Croyal, M., Bouzelha, M., Mével, M., Deniaud, D., Boujtita, M., Gouin, S.G., 2018. J. Am. Chem. Soc. 140 (49), 17120–17126.
Cardona Maya, W.D., Du Plessis, S.S., Velilla, P.A., 2020. Reprod. Biomed. Online 40 (6), 763–764.
Chen, F., Lou, D., 2020. Urology 142, 42.
Di Trani, M., Mariani, R., Ferri, R., De Berardinis, D., Frigo, M.G., 2021. Front. Psychol. 12 (987).
Drobysh, M., Ramanaviciene, A., Viter, R., Ramanavicius, A., 2021. Micromachines 12 (4), 390.
Dronina, J., Bubniene, U.S., Ramanavicius, A., 2021. Biosens. Bioelectron. 175, 112867.
Feingold, J.H., Peccoralo, L., Chan, C.C., Kaplan, C.A., Kaye-Kauderer, H., Charney, D., Verity, J., Hurtado, A., Burka, L., Syed, S.A., Murrough, J.W., Feder, A., Pietrzak, R. H., Ripp, J., 2021. Chronic Stress 5, 2470547020977891.
García-Miranda Ferrari, A., Rowley-Neale, S.J., Banks, C.E., 2021. Talanta Open 3, 100032.
Gheblawi, M., Wang, K., Viveiros, A., Nguyen, Q., Zhong, J.-C., Turner, A.J., Raizada, M. K., Grant, M.B., Oudit, G.Y., 2020. Circ. Res. 126 (10), 1456–1474.
Guney, C., Akar, F., 2021. J. Pharm. Pharmaceut. Sci. 24, 84–93.
Huang, L., Sexton, D.J., Skogerson, K., Devlin, M., Smith, R., Sanyal, I., Parry, T., Kent, R., Enright, J., Wu, Q.-l., Conley, G., DeOliveira, D., Morganelli, L., Ducar, M., Wescott, C.R., Ladner, R.C., 2003. J. Biol. Chem. 278 (18), 15532–15540.
La Marca, A., Busani, S., Donno, V., Guaraldi, G., Ligabue, G., Girardis, M., 2020. Reprod. Biomed. Online 41 (5), 903–906.
Larios, J.M., Budhiraja, R., Fanburg, B.L., Thannickal, V.J., 2001. J. Biol. Chem. 276 (20), 17437–17441.
Li, H., Xiao, X., Zhang, J., Zafar, M.I., Wu, C., Long, Y., Lu, W., Pan, F., Meng, T., Zhao, K., Zhou, L., Shen, S., Liu, L., Liu, Q., Xiong, C., 2020a. EClinicalMedicine 28.
Li, R., Yin, T., Fang, F., Li, Q., Chen, J., Wang, Y., Hao, Y., Wu, G., Duan, P., Wang, Y., Cheng, D., Zhou, Q., Zafar, M.I., Xiong, C., Li, H., Yang, J., Qiao, J., 2020b. Reprod. Biomed. Online 41 (1), 89–95.
Ma, X., Guan, C., Chen, R., Wang, Y., Feng, S., Wang, R., Qu, G., Zhao, S., Wang, F., Wang, X., Zhang, D., Liu, L., Liao, A., Yuan, S., 2021. Cell. Mol. Immunol. 18 (2), 487–489.
Mehta, S., Machado, F., Kwizera, A., Papazian, L., Moss, M., Azoulay, É., Herridge, M., 2021. The Lancet Respiratory Medicine 9 (3), 226–228.
Morgantini, L.A., Naha, U., Wang, H., Francavilla, S., Acar, Ö., Flores, J.M., Crivellaro, S., Moreira, D., Abern, M., Eklund, M., Vigneswaran, H.T., Weine, S.M., 2020. PLoS One 15 (9), e0238217.
Nagy Jr., B., Fejes, Z., Szentkereszty, Z., Sütő, R., Várkonyi, I., Ajzner, É., Kappelmayer, J., Papp, Z., Tóth, A., Fagyas, M., 2021. Int. J. Infect. Dis. 103, 412–414.
Patrì, A., Gallo, L., Guarino, M., Fabbrocini, G., 2020. J. Am. Acad. Dermatol. 82 (6), e227.
Permentier, H.P., Bruins, A.P., 2004. J. Am. Soc. Mass Spectrom. 15 (12), 1707–1716.
Plikusiene, I., Maciulis, V., Ramanaviciene, A., Balevicius, Z., Buzavaite-Verteliene, E., Ciplys, E., Slibinskas, R., Simanavicius, M., Zvirbliene, A., Ramanavicius, A., 2021. J. Colloid Interface Sci. 594, 195–203.
Prasad, K., McLoughlin, C., Stillman, M., Poplau, S., Goelz, E., Taylor, S., Nankivil, N., Brown, R., Linzer, M., Cappelucci, K., Barbouche, M., Sinsky, C.A., 2021. EClinicalMedicine 35.
Sasangohar, F., Jones, S.L., Masud, F.N., Vahidy, F.S., Kash, B.A., 2020. Anesth. Analg. 131 (1), 106–111.
Sungnak, W., Huang, N., Bécavin, C., Berg, M., Queen, R., Litvinukova, M., Talavera-López, C., Maatz, H., Reichart, D., Sampaziotis, F., Worlock, K.B., Yoshida, M., Barnes, J.L., Banovich, N.E., Barbry, P., Brazma, A., Collin, J., Desai, T.J., Duong, T. E., Eickelberg, O., Falk, C., Farzan, M., Glass, I., Gupta, R.K., Haniffa, M., Horvath, P., Hubner, N., Hung, D., Kaminski, N., Krasnow, M., Kropski, J.A., Kuhnemund, M., Lako, M., Lee, H., Leroy, S., Linnarson, S., Lundeberg, J., Meyer, K. B., Miao, Z., Misharin, A.V., Nawijn, M.C., Nikolic, M.Z., Noseda, M., Ordovas-Montanes, J., Oudit, G.Y., Pe'er, D., Powell, J., Quake, S., Rajagopal, J., Tata, P.R., Rawlins, E.L., Regev, A., Reyfman, P.A., Rozenblatt-Rosen, O., Saeb-Parsy, K., Samakovlis, C., Schiller, H.B., Schultze, J.L., Seibold, M.A., Seidman, C.E., Seidman, J.G., Shalek, A.K., Shepherd, D., Spence, J., Spira, A., Sun, X., Teichmann, S.A., Theis, F.J., Tsankov, A.M., Vallier, L., van den Berge, M., Whitsett, J., Xavier, R., Xu, Y., Zaragosi, L.-E., Zerti, D., Zhang, H., Zhang, K., Rojas, M., Figueiredo, F., Network, H.C.A.L.B., 2020. Nat. Med. 26 (5), 681–687.
Theorell, T., 2020. Psychother. Psychosom. 89 (4), 193–194.
Vandenberg, O., Martiny, D., Rochas, O., van Belkum, A., Kozlakidis, Z., 2021. Nat. Rev. Microbiol. 19 (3), 171–183.
Zafar, M.I., Li, H., 2020. EClinicalMedicine 29.